

Spin-disorder resistivity of random fcc-NiFe alloys

V. Drchal and J. Kudrnovský

Institute of Physics, Academy of Sciences of the Czech Republic, Na Slovance 2, CZ-182 21 Prague 8, Czech Republic

D. Wagenknecht

*Department of Condensed Matter Physics, Faculty of Mathematics and Physics, Charles University,
Ke Karlovu 5, CZ-121 16 Prague, Czech Republic*

I. Turek

*Institute of Physics of Materials, Academy of Sciences of the Czech Republic, Žitkova 22,
CZ-616 62 Brno, Czech Republic*

(Received 9 July 2018; revised manuscript received 17 September 2018; published 24 October 2018)

The spin-disorder resistivity (SDR) of a disordered fcc-(Ni_{1-x}, Fe_x) alloy is determined from first principles. We identify the SDR at and above the critical temperature with the residual resistivity of the corresponding paramagnetic state evaluated in the framework of the disordered local moment (DLM) model. The underlying electronic structure is determined by means of the tight-binding linear muffin-tin orbital method, which employs the coherent potential approximation (CPA) to describe both the DLM state and the chemical disorder in alloys. An extension of the DLM fixed-spin moment method for two independent magnetic moments is used and combined with the paramagnetic lattice gas entropy to determine local moments by minimizing the corresponding free energy. The effect of phonon scattering is included through the mapping of static atomic displacements into a multicomponent random alloy which is then treated in the CPA. Finally, the Kubo-Greenwood-CPA approach is employed to estimate the SDR. We also address the problem of the validity of the Matthiessen rule at the Curie point. Good agreement of calculated and measured SDR is obtained over the whole studied concentration range; the results point to the importance of nonzero Ni magnetic moments in the limit of pure nickel.

DOI: [10.1103/PhysRevB.98.134442](https://doi.org/10.1103/PhysRevB.98.134442)**I. INTRODUCTION**

The temperature dependence of resistivity is one of the basic properties of any metallic system. In particular, in magnetic metals, in addition to the conventional residual resistivity due to impurities ρ_{imp} and the contribution due to scattering on phonons ρ_{ph} or static displacements of atomic nuclei, an additional scattering mechanism due to spin fluctuations ρ_{sf} also exists. It usually reaches its maximum close to the corresponding critical temperature (Curie temperature T_C in the present case) and remains constant above it. The latter, the spin-disorder part of the resistivity (SDR), is an important characteristic of the paramagnetic state, and it is the main subject of this paper. The SDR is also readily available from the experiment: one measures the low-temperature resistivity or ρ_{imp} and resistivity well above critical temperature, where ρ_{ph} varies linearly [1] with temperature T while ρ_{sf} remains constant. The SDR is then obtained by extrapolating the linear dependence of ρ_{ph} at high temperatures above T_C down to $T = 0$ and subtracting ρ_{imp} , as illustrated in Fig. 1. Clearly, this is an approximate approach which assumes the validity of the Matthiessen rule: if one neglects the many-body effects, the total resistivity is expressed as

$$\rho_{\text{tot}} = \rho_{\text{imp}} + \rho_{\text{ph}} + \rho_{\text{sf}}. \quad (1)$$

As shown by Fert and Campbell [2], the temperature dependence of the resistivity can be affected by deviations from the Matthiessen rule due to the presence of two spin channels for conduction. We therefore also investigate the validity of the Matthiessen rule at the Curie temperature. It should be noted that the evaluation of the SDR is a simpler problem than the estimate of the resistivity over the whole temperature range because at and above T_C the contribution due to spin fluctuations is constant.

There were numerous attempts in the past to estimate resistivity due to spin fluctuations on a model level (based on the s - d model Hamiltonian; see, e.g., Refs. [3–6]). A quantitative description of the SDR using first-principles calculations was not attempted until recently. We mention Ref. [7] for the estimate of the SDR of elemental ferromagnets Ni and Fe and Ref. [8], in which several ferromagnets, mostly ordered ones, were studied.

Systematic first-principles estimates of the SDR for disordered alloys are still missing in the literature. In the present study we wish to fill in this gap by choosing as a case study the disordered fcc-(Ni_{1-x}, Fe_x) alloy for which extensive experimental data also exist [9]. This system is also interesting theoretically because important longitudinal spin fluctuations on one of the alloy constituents (Ni) exist. We therefore develop a corresponding formal theory to estimate the SDR in such alloys.

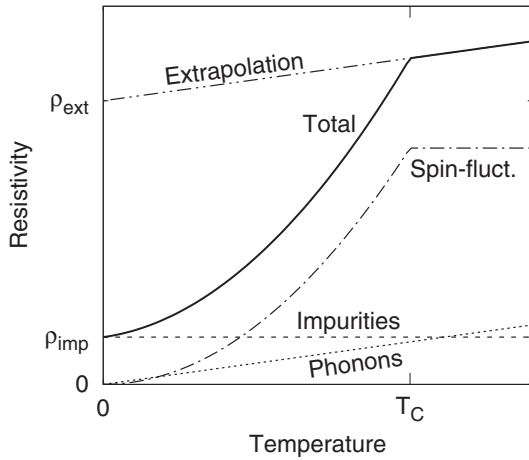


FIG. 1. The schematic illustration of the temperature-dependent resistivity and its main contributions due to impurities, phonons, and spin fluctuations which assumes the validity of the Matthiessen rule. How the SDR is determined experimentally from the ρ_{ext} found by extrapolation from the high-temperature region and the residual (impurity) resistivity ρ_{imp} as $\rho_{\text{SDR}} = \rho_{\text{ext}} - \rho_{\text{imp}}$ is also shown.

II. FORMALISM

The evaluation of the SDR requires us to answer two questions, namely, (i) how to describe the paramagnetic state and (ii) how to evaluate its resistivity [8]. We approximate the paramagnetic state by the disordered local moment (DLM) model as an uncorrelated ensemble of randomly oriented spins with zero total magnetic moment. It can be treated in the coherent potential approximation (CPA) as an equiconcentration binary alloy of atoms with moments up (\uparrow) and with moments down (\downarrow) [10]. More specifically, in the present alloy model with two types of magnetic atoms we have a four-component alloy, namely, fcc-($\text{Ni}_{(1-x)/2}^{\uparrow}, \text{Ni}_{(1-x)/2}^{\downarrow}, \text{Fe}_{x/2}^{\uparrow}, \text{Fe}_{x/2}^{\downarrow}$). This approach is implemented in the framework of the scalar-relativistic tight-binding linear muffin-tin orbital (TB-LMTO) method [11] and the local-density approximation [12]. We employ the *spdf* basis and the same atomic sphere radii of alloy constituents. We also neglect small changes in the lattice constant due to both alloying and temperature, which also depend on the alloy annealing. We have chosen as a reference value the lattice constant of permalloy.

The DLM local moment collapses to zero in some cases, e.g., fcc-Ni, the local Ni moment in fcc-($\text{Ni}_{1-x}, \text{Fe}_x$), and bcc-Fe in Earth's core conditions. The fluctuating moment can be, nevertheless, stabilized even in these cases by the magnetic entropy effects [13–15] and can be estimated from the minimization of the free energy, which contains the randomness of the local-moment directions and longitudinal spin fluctuations. In numerical calculations we employ the fixed-spin moment (FSM) method [16,17] applied to the DLM state [18]. The local magnetic moments are treated as independent variables, and total energy is calculated for prescribed values of moments. The specific form of the magnetic entropy which enters the free-energy expression is still under discussion. We employ the entropy of a paramagnetic lattice gas ($S \propto \ln(1+m)$, see Refs. [19,20], which is sometimes connected

with the names of Heine and Joynt [21] and Grimvall [22]). It is a good approximation if the thermal energy of the moment is considerably larger than the energy of its interaction with the neighborhood. This is the situation in the DLM state [20].

The fcc-NiFe alloy studied here is complicated due to the presence of two moments which behave differently; namely, Ni moments exhibit pronounced longitudinal fluctuations, while the Fe moments are rather rigid. We have therefore extended the formalism which was successfully used for pure metals (fcc-Ni and bcc-Fe at the Earth's core conditions [15]) to the case of two local moments, and we allow for longitudinal fluctuations on both Ni and Fe atoms. We refer the reader to the Appendix for details.

The SDR itself is then determined by the linear-response theory as formulated in the framework of the TB-LMTO method using the Kubo-Greenwood-CPA formula [23] applied to the DLM state. In the present cubic system, the SDR equals the calculated diagonal elements of the resistivity tensor $\rho_{\mu,\nu}$, i.e., $\text{SDR} = \rho_{xx} = \rho_{yy} = \rho_{zz}$. The disorder-induced vertex corrections [24], which describe the correlated motion of two electrons in a random alloy potential, are also included. Their inclusion is simplified by the present formulation of the velocity as the intersite hopping [23], which leads to nonrandom effective velocity matrices. Such formulation relies on the neglect of electron motion inside atomic spheres, and it is an excellent approximation in the limit of the static linear response regime used here.

The inclusion of temperature-induced static displacements of atoms (phonons) in resistivity calculations is similar in spirit to the approach developed within the Korringa-Kohn-Rostoker-CPA technique [25]. Here we apply it in the framework of the TB-LMTO-CPA method [26,27]. This scheme assumes static random displacements of the atomic nuclei around the equilibrium positions (sites of an ideal crystalline lattice). The change in the LMTO structure-constant matrix due to the atomic displacements can be recast into a change in the potential parameters of atoms located formally at the sites of the undistorted crystalline lattice, which are then treated using the multicomponent CPA. Correlations between the displacements of neighboring atoms are neglected. Theory depends on an external parameter, namely, on the rms deviations which characterize the effect of temperature. The temperature dependence of rms deviations either is empirical or is determined explicitly on the basis of a simple Debye-Grüneisen model [1]. The formalism developed originally for transition metals is extended here to random alloys. In principle, deviations of individual atoms in alloy are different. Here we used one common rms deviation, which is an acceptable approximation due to similar masses of Ni and Fe. It is important to note that the present formulation allows us to treat all involved scattering mechanisms (chemical disorder, atomic displacements, and spin fluctuations) on equal footing in the framework of the CPA.

In conclusion we mention also an alternative approach for the estimate of the SDR which is based on the Kubo-Landauer approach which employs the direct averaging over spin-disordered supercells and which also allows us to include the effect of phonons [7,28]. Until now it was applied to only ordered crystals.

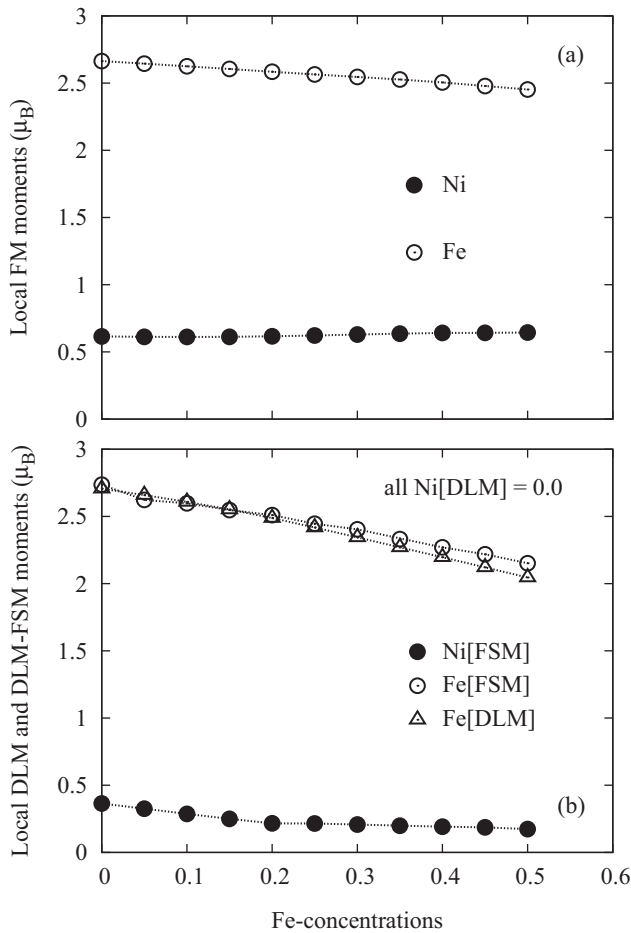


FIG. 2. The local Ni (solid circles) and Fe (open circles) magnetic moments for the disordered fcc-(Ni_{1-x}, Fe_x) alloy as a function of the Fe concentration: (a) calculated in the FM state and (b) calculated in the DLM state without and with the FSM method. Local Ni moments collapse to zero for all concentrations in the DLM state and are not shown. The DLM-FSM values for $x_{Fe} = 0.05$ and 0.35 were obtained with the help of interpolated experimental values [9] of T_C for $x_{Fe} = 0.0$ and 0.1 and $x_{Fe} = 0.3$ and 0.4 , respectively.

III. RESULTS AND DISCUSSION

A. Local magnetic moments in fcc-(Ni_{1-x}, Fe_x)

Local magnetic moments are basic quantities in magnetic alloys. It should be noted that the local moments depend slightly on the division of space between Ni and Fe atoms. Space-filling spheres with the same radii for both components are used here. The NiFe alloy has the fcc structure for $x_{Fe} \leq 0.5$. In Fig. 2 we present calculated local moments as a function of the iron concentration used in the SDR experiment. We show, in addition to DLM-FSM moments, local moments in the ferromagnetic (FM) state (at temperature $T = 0$) and also those for the conventional DLM state. The following conclusions can be made: (i) In the FM state [Fig. 2(a)] local Ni moments are essentially concentration independent, while the local Fe moments decrease weakly with increasing Fe content. As a result, we obtain an almost linear increase of the average magnetization from the value of about $0.6\mu_B$ for pure fcc-Ni. This is in agreement with the experiment [29].

(ii) The calculated local Ni moments in the DLM state collapse to zero over the whole concentration range. This would yield zero SDR for pure fcc-Ni, in contradiction to experiment, which gives nonzero SDR. The DLM-FSM method leads to fluctuating local Ni moments stabilized by the magnetic entropy, while the local Fe moments are essentially the same as those obtained from the DLM method. However, their decrease with increasing Fe content is larger than in the FM state. The local Ni moment in the DLM-FSM state is close to $0.4\mu_B$ for pure fcc-Ni and weakly decreases with x_{Fe} being essentially constant for $x_{Fe} > 0.2$. The value of the local Ni moment for pure fcc-Ni obtained in the framework of the DLM-FSM method agrees with the experiment [30]. We also include the DLM-FSM results for $x_{Fe} = 0.05$ and 0.35 , for which the experimental T_C are not given in Ref. [9]. The linear extrapolation was used for these T_C in the present study.

B. SDR in fcc-(Ni_{1-x}, Fe_x)

1. The effect of alloy composition

We have calculated the SDR for DLM- and DLM-FSM models as a function of the Fe content and summarize the results in Figs. 3(a) and 3(b), respectively. We present calculated SDR together with experimental results [9]. The following conclusions can be made: (i) The SDR is about $15 \mu\Omega \text{ cm}$ for pure fcc-Ni ($x_{Fe} = 0$), in agreement with the experiment (see, e.g., Ref. [8]). It should be noted that the choice of the DLM-FSM model for a correct value of the SDR is relevant, as shown below. (ii) The experiment shows a monotonic increase of the SDR as a function of the Fe content. The wiggly shape of this dependence is most likely due to the sample preparation, like annealing, a tendency to ordering close to $x_{Fe} = 0.25$ or 0.5 , etc. (iii) The monotonic increase in the SDR with increasing x_{Fe} is due to the increasing amount of strong spin-disorder scatterings on Fe sites (because of large d -level splitting or large local magnetic moments) compared to Ni sites. (iv) The SDR-DLM-FSM calculations agree with the experiment in detail. In particular, three concentration regions, two with smaller slope [$x_{Fe} = (0, 0.15)$ and $(0.30, 0.50)$] and the other [$x_{Fe} = (0.15, 0.30)$] with larger slope, agree well with the experiment. (v) The observed saturation of the concentration dependence of the SDR is due to the Nordheim-like behavior; that is, the scattering is largest around the equiconcentration case. (vi) Finally, the results of the SDR-DLM calculations are shown in Fig. 3(a) for comparison. Although an increase of the SDR with Fe content is obtained also in this model, its agreement with experiment is much worse than in the DLM-FSM case [Fig. 3(b)], in particular for the Ni-rich case. Specifically, the SDR is zero for pure Ni. Such disagreement has to be expected because local Ni moments collapse to zero in the DLM case. The agreement with the experiment improves with increasing Fe concentration.

2. The effect of ordering and relativistic effects

We have investigated the effect of the spin-orbit coupling on the SDR by using alloys with $x_{Fe} = 0.25$ and 0.50 as case studies. To this end we have employed the fully relativistic transport codes [31] under simplifying conditions: (i) Only the

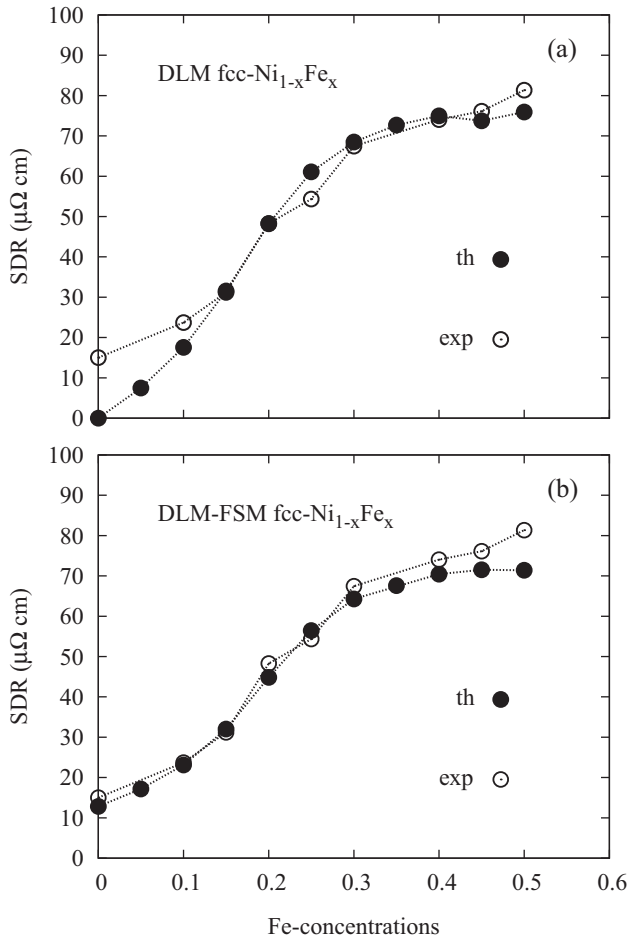


FIG. 3. Calculated SDR (solid circles) for disordered fcc-(Ni_{1-x}, Fe_x) as a function of the Fe concentration: (a) the DLM method and (b) the DLM-FSM method. Theoretical (th) results are compared with the experiment [9] (exp) in both cases. No experimental data are available for $x_{\text{Fe}} = 0.05$ and 0.35 concentrations.

DLM, not the DLM-FSM, input is used, and (ii) we describe the relativistic DLM with the help of a 50:50 random alloy, as in the scalar-relativistic limit, rather than use a more accurate multiconcentration model. We showed in Ref. [8] that this is an acceptable approximation for light metals like Fe and Ni. Finally, the effect of alloy ordering was investigated for two existing superstructures, namely, $L1_2$ Ni₃Fe and $L1_0$ NiFe. The $L1_2$ Ni₃Fe preserves its cubic symmetry for components of the resistivity tensor, while for the $L1_0$ NiFe alloy there are different values of the SDR for components parallel and normal to the Ni and Fe planes. In Table I we present only average values. It should be noted, however, that we speak about alloys ordered chemically but not magnetically, with the present strong spin disorder due to the Fe spin fluctuations. The results are compared with their disordered counterparts ($x_{\text{Fe}} = 0.25$ and 0.50). All results are summarized in Table I with the following conclusions: (i) The reference disordered fcc-NiFe alloy ($x_{\text{Fe}} = 0.25$) has slightly larger SDR for the model which neglects Ni spin fluctuations (values in parentheses). Such a result comes from a competition of two effects, namely, missing weak disorder on Ni sites (which should

TABLE I. Calculated reference scalar-relativistic SDR values for disordered fcc-(Ni₇₅, Fe₂₅) and fcc-(Ni₅₀, Fe₅₀) alloys are compared with corresponding ordered $L1_2$ Ni₃Fe and $L1_0$ NiFe alloys, respectively. Two different model potentials were used for ordered alloys, namely, those constructed (i) from the DLM-FSM potentials of corresponding disordered alloys and (ii) from the DLM potentials of disordered alloys (shown in parentheses). The local Ni moments collapse to zero in this model. Finally, we include for completeness the fully relativistic SDR for disordered samples based on a simple DLM model (see text for details). The local Ni moments collapse to zero also in the relativistic limit.

x_{Fe}	SDR ($\mu\Omega \text{ cm}$)			
	Reference	$L1_2$ Ni ₃ Fe	$L1_0$ NiFe	Dirac
0.25	56.5 (61.1)	45.4 (17.7)		(71.8)
0.50	71.4 (75.9)		73.0 (99.0)	(79.0)

decrease the SDR) and a smaller density of states (DOS) at the Fermi energy E_F (proportional to the number of carriers at E_F) which should increase the SDR. Specifically, $\text{DOS}(E_F)$ amounts to 10.85 and 11.77 states/Ry for the DLM and DLM-FSM cases, respectively. (ii) We note a smaller SDR for the ordered DLM-Ni₃Fe alloy compared to that for the case of a disordered counterpart treated with the DLM-FSM method. It is a result of missing scattering on Ni sites (we have three ideal, unperturbed Ni sublattices in the DLM model), and the spin disorder is present only on the Fe sublattice. (iii) The SDR of $L1_0$ NiFe calculated using the DLM input is larger than the SDR calculated from the input taken from the disordered counterpart because the local Fe moment is larger in the ordered phase than in the disordered one ($2.40\mu_B$ vs $2.15\mu_B$). The Fe moment is a much stronger scatterer than the Ni moment. We illustrate the SDR anisotropy for $L1_0$ NiFe alloys using the DLM-FSM input: $\rho_{\text{sf}} = 64.76 \mu\Omega \text{ cm}$ and $\rho_{\text{sf}} = 89.42 \mu\Omega \text{ cm}$ for current parallel and normal to the Ni and Fe planes, respectively. Similar results are obtained also for the DLM input. (iv) The spin-orbit coupling slightly enhances the SDR value similarly, as was found previously for the bcc-Fe case [8]. The reason is mixing of spin channels in the relativistic theory.

C. The Matthiessen rule

The experimental studies of the SDR are based on the assumption of the validity of the Matthiessen rule (MR), Eq. (1). We have therefore, for consistency, calculated the SDR in the same limit. There exist, however, metals for which the MR rule is not valid. Let us mention at least two recent examples, namely, the hcp-Gd [32] and the bcc-Fe under Earth's core conditions [15].

We study the validity of the MR by evaluating the total resistivity of disordered fcc-(Ni_{1-x}, Fe_x) alloys in two models to which we add the effect of phonons: (i) an alloy with the presence of only impurities (imp+ph) and (ii) an alloy which includes the effect of impurities and spin fluctuations (imp+ph+sf). The validity of the MR for phonons can be thus checked. As discussed above, an advantage of the present approach is the inclusion of all listed types of

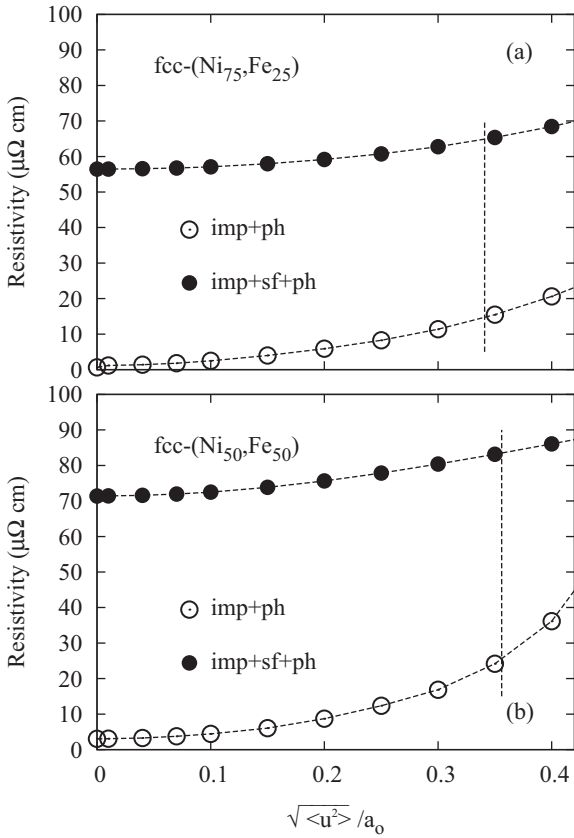


FIG. 4. The validity of the Matthiessen rule: (a) The resistivity of the fcc-(Ni₇₅, Fe₂₅) alloy as a function of the rms displacement $\sqrt{\langle u^2 \rangle}$. The label “imp+ph” (open circles) denotes the model in which impurities (imp) and static displacements (ph, phonons) are present, while the label “imp+sf+ph” (solid circles) denotes the model in which spin fluctuations (sf) are also present. All types of disorder are treated on the same footing by using the multicomponent CPA. (b) The same as in (a), but for the fcc-(Ni₅₀, Fe₅₀) alloy. The long vertical lines indicate the rms displacement at T_C estimated from the Debye theory [1,33].

scattering mechanisms on equal footing in the framework of the multicomponent CPA approach [15,32]. We closely follow the approach adopted in Ref. [15] and evaluate the total resistivity of alloys for models (i) and (ii) as a function of the rms displacements or, indirectly, as a function of temperature. The rms displacements can be related approximately to temperature on the basis of the Debye theory [33]. Results are summarized in Figs. 4(a) and 4(b) with two conclusions: (i) There is a monotonic increase of the total resistivity with the rms displacement which amounts to almost 10 and 20 $\mu\Omega$ cm at T_C for fcc-(Ni₇₅, Fe₂₅) and fcc-(Ni₅₀, Fe₅₀), respectively. (ii) The resistivity in the imp+ph case increases with the rms displacement slightly more than in the case of imp+ph+sf, indicating a weak violation of the MR in both cases, a stronger one for the fcc-(Ni₅₀, Fe₅₀) alloy.

IV. CONCLUSIONS

We have developed the first-principles approach to estimate the SDR for alloys when longitudinal spin fluctuations are

relevant. We have determined the magnetic moments and potentials by minimizing the free energy, in which the fluctuating moment directions and the longitudinal spin fluctuations are described by the DLM-FSM method and the magnetic entropy has a form corresponding to a paramagnetic lattice gas. The developed theory was applied to the case of fcc-(Ni_{1-x}, Fe_x) alloys. The main conclusions are as follows: (i) There is very good agreement between the theoretical and experimental values of the SDR. (ii) The model neglecting longitudinal spin fluctuations fails in the Ni-rich region, but it gives an acceptable description for larger Fe content where scattering on Fe moments dominates. (iii) The MR is only weakly violated with increasing temperature, and its violation is larger for higher Fe concentrations.

ACKNOWLEDGMENTS

This work is supported by a grant from the Czech Science Foundation (Grant No. 18-07172S). One of us (D.W.) acknowledges the support from the National Grid Infrastructure MetaCentrum (project CESNET LM2015042) and the Ministry of Education, Youth and Sports (project LM2015070).

APPENDIX: FLUCTUATING LONGITUDINAL MAGNETIC MOMENTS

Local magnetic moments in metallic systems usually do not disappear at and above the Curie temperature, but they rather acquire random orientations, so that the total magnetization becomes zero (the paramagnetic state). This state can be described using the disordered local moments [10]. It has been shown that it is equivalent to an equiconcentration binary alloy of atoms with moments up (50%) and with moments down (50%). The binary alloy Ni_{1-x}Fe_x in the DLM state is then equivalent to a four-component alloy, Ni_{(1-x)/2}[↑]Ni_{(1-x)/2}[↓]Fe_{x/2}[↑]Fe_{x/2}[↓]. Various methods to find thermodynamical equilibrium are described in the literature. Here we look for the minimum of the free energy per site,

$$F(m_1, m_2, T) = E_{\text{tot}}(m_1, m_2) - T[(1-x)S(m_1) + xS(m_2)], \quad (\text{A1})$$

where the magnetic moments m_1 and m_2 of the alloy species are expressed in Bohr magnetons μ_B . We employ the entropy of a paramagnetic lattice gas [19,20],

$$S(m) = k_B \ln(1 + m), \quad (\text{A2})$$

which is a good approximation if the thermal energy of the moment is considerably larger than its interaction energy with the rest of the system as it is in the DLM state. This approach was successfully used in several studies of materials with disordered local moments [20,34–36]. For further discussion see Ref. [37].

The calculation of the electronic structure yields magnetic moments m_1^0 and m_2^0 , corresponding to a minimum of total energy. At nonzero temperature the entropic effect leads to different moments m_1 and m_2 that minimize the free energy (A1). In order to calculate these moments we need to know the total energy $E_{\text{tot}}(m_1, m_2)$ as a function of moments m_1 and m_2 . It can be obtained using the fixed-spin moment (FSM) method [16,17] extended to the DLM state [18], which allows

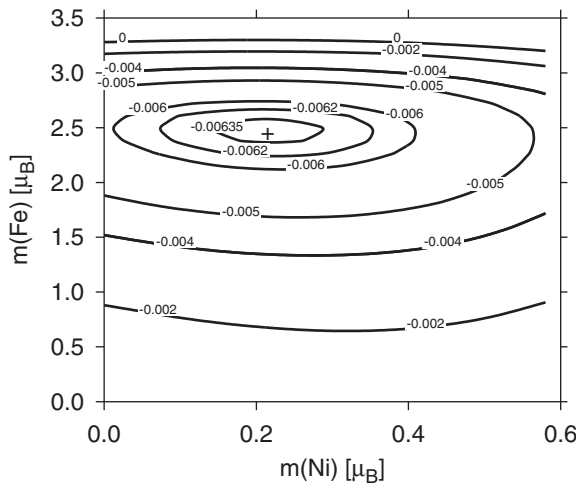


FIG. 5. Magnetic part of the free energy of the fcc-(Ni₇₅, Fe₂₅) alloy as a function of averaged local magnetic moments $m(\text{Ni})$ and $m(\text{Fe})$ on Ni and Fe atoms at the Curie temperature (850 K). The numbers attached to isolines are values of the free energy in Ry units. The cross indicates the position of the free-energy minimum. The corresponding local moments are then $0.22\mu_{\text{B}}$ and $2.45\mu_{\text{B}}$ for Ni and Fe, respectively.

us to describe the longitudinal moment fluctuations. Original formulation of the FSM method was based on auxiliary magnetic fields that split up- and down-spin subbands. It turned out, however, that the magnetic moments are often

multivalued functions of applied fields [16,17], which leads to nonphysical results. The solution is to prescribe moments [38] and introduce several Fermi energies (for each alloy species and for each spin orientation). In our case there are four Fermi energies, namely, Ni^\uparrow , Ni^\downarrow , Fe^\uparrow , and Fe^\downarrow , and we require that magnetic moments have values m_1 and m_2 ; the total number of electrons per site is $n = (1-x)n(\text{Ni}) + xn(\text{Fe})$, and the charge transfer between Ni and Fe atoms has a prescribed value. In this work we assume that charge transfer is identical to that found from the total-energy minimization. We note that the minimum of the free energy $F(m_1, m_2)$ and moments m_1 and m_2 can be found in a single self-consistent calculation if the entropic term is added to the energy functional [20]. In our case the elementary cell contains only one atom, so the calculations are not demanding. We thus made calculations for a grid of moments, which gives the possibility to inspect the energy surface for the presence of other minima.

In calculations of transport properties a single, common Fermi energy is needed. Within the LMTO method it can be selected arbitrarily, but the potential parameters C and E_v of all alloy species have to be shifted accordingly. We illustrate the above approach for the case of disordered fcc-(Ni₇₅, Ni₂₅) alloys (see Fig. 5). Figure 5 shows contours of constant free energy (energy values are attached to isolines) around the free-energy minimum corresponding to the Curie temperature (850 K). Estimated local Ni and Fe moments are $0.24\mu_{\text{B}}$ and $2.54\mu_{\text{B}}$, respectively. Corresponding potentials then serve as an input for transport calculations. A similar approach is also used for other iron concentrations.

-
- [1] J. M. Ziman, *Electrons and Phonons* (Oxford University Press, Oxford, 1960).
- [2] A. Fert and I. A. Campbell, *Phys. Rev. Lett.* **21**, 1190 (1968).
- [3] T. Kasuya, *Prog. Theor. Phys.* **16**, 58 (1956).
- [4] T. Kasuya, *Prog. Theor. Phys.* **22**, 227 (1959).
- [5] P. G. de Gennes and J. Friedel, *J. Phys. Chem. Solids* **4**, 71 (1958).
- [6] M. E. Fisher and J. S. Langer, *Phys. Rev. Lett.* **20**, 665 (1968).
- [7] A. Wysocki, K. D. Belashchenko, and J. P. Velev, *J. Appl. Phys.* **101**, 09G506 (2007).
- [8] J. Kudrnovský, V. Drchal, I. Turek, S. Khmelevskiy, J. K. Glasbrenner, and K. D. Belashchenko, *Phys. Rev. B* **86**, 144423 (2012).
- [9] S. U. Jen and S. S. Liou, *J. Appl. Phys.* **85**, 8217 (1999).
- [10] B. L. Gyorffy, A. J. Pindor, J. Staunton, G. M. Stocks, and H. Winter, *J. Phys. F* **15**, 1337 (1985).
- [11] I. Turek, V. Drchal, J. Kudrnovský, M. Šob, and P. Weinberger, *Electronic Structure of Disordered Alloys, Surfaces and Interfaces* (Kluwer, Boston, 1997).
- [12] S. H. Vosko, L. Wilk, and M. Nusair, *Can. J. Phys.* **58**, 1200 (1980).
- [13] A. V. Ruban, S. K. Khmelevskiy, P. Mohn, and B. Johansson, *Phys. Rev. B* **75**, 054402 (2007).
- [14] A. V. Ruban, A. B. Belonoshko, and N. V. Skorodumova, *Phys. Rev. B* **87**, 014405 (2013).
- [15] V. Drchal, J. Kudrnovský, D. Wagenknecht, I. Turek, and S. Khmelevskiy, *Phys. Rev. B* **96**, 024432 (2017).
- [16] K. Schwartz and P. Mohn, *J. Phys. F* **14**, L129 (1984).
- [17] V. L. Moruzzi, P. M. Marcus, K. Schwarz, and P. Mohn, *Phys. Rev. B* **34**, 1784 (1986).
- [18] V. Drchal, J. Kudrnovský, and I. Turek, *EPJ Web Conf.* **40**, 11001 (2013).
- [19] R. J. Weiss and K. J. Tauer, *Phys. Rev.* **102**, 1490 (1956).
- [20] H. Ehteshami and P. A. Korzhavyi, *Phys. Rev. B* **96**, 224406 (2017).
- [21] V. Heine and R. Joynt, *Europhys. Lett.* **5**, 81 (1988).
- [22] G. Grimvall, *Phys. Rev. B* **39**, 12300 (1989).
- [23] I. Turek, J. Kudrnovský, V. Drchal, L. Szunyogh, and P. Weinberger, *Phys. Rev. B* **65**, 125101 (2002).
- [24] K. Carva, I. Turek, J. Kudrnovský, and O. Bengone, *Phys. Rev. B* **73**, 144421 (2006).
- [25] H. Ebert, S. Mankovsky, K. Chadova, S. Polesya, J. Minár, and D. Ködderitzsch, *Phys. Rev. B* **91**, 165132 (2015).
- [26] D. Wagenknecht, K. Carva, and I. Turek, *Proc. SPIE* **10357**, 103572W (2017).
- [27] D. Wagenknecht, K. Carva, and I. Turek, *IEEE Trans. Magn.* **53**, 1700205 (2017).
- [28] A. A. Starikov, Y. Liu, Z. Yuan, and P. J. Kelly, *Phys. Rev. B* **97**, 214415 (2018).
- [29] G. Blaise and M. C. Cadeville, *J. Phys.* **35**, 545 (1975).
- [30] M. Acet, E. F. Wassermann, K. Andersen, A. Murani, and O. Scharpf, *Europhys. Lett.* **40**, 93 (1997).

- [31] I. Turek, J. Kudrnovský, and V. Drchal, *Phys. Rev. B* **89**, 064405 (2014).
- [32] J. K. Glasbrenner, B. S. Pujari, and K. D. Belashchenko, *Phys. Rev. B* **89**, 174408 (2014).
- [33] Y. Tanji, *J. Phys. Soc. Jpn.* **30**, 133 (1971).
- [34] L. Vitos, P. A. Korzhavyi, and B. Johansson, *Phys. Rev. Lett.* **96**, 117210 (2006).
- [35] V. I. Razumovskiy, A. V. Ruban, and P. A. Korzhavyi, *Phys. Rev. Lett.* **107**, 205504 (2011).
- [36] D. Ma, B. Grabowski, F. Körman, J. Neugebauer, and D. Raabe, *Acta Mater.* **100**, 90 (2015).
- [37] S. Khmelevskiy, *J. Magn. Magn. Mater.* **461**, 14 (2018).
- [38] P. H. Dederichs, S. Blügel, R. Zeller, and H. Akai, *Phys. Rev. Lett.* **53**, 2512 (1984).